Recent Advances in Micro/Nano-Structured Heat Pipes

Yihao ZHANG[a], Jinwang LI[a,b,*], Zhen ZHANG[a]

[a]College of Astronautics, Nanjing University of Aeronautics and Astronautics, Nanjing 211106, China

[b]Key Laboratory of Aero-engine Thermal Environment and Structure, Ministry of Industry and Information Technology, Nanjing, China

Corresponding author; E-mail: ljw@nuaa.edu.cn

The development of high-performance and high-density packaging electronic devices has led to the concentration of heat generation in smaller areas, resulting in the formation of "hotspots", i.e., regions of high heat flux. Localized high temperatures can adversely affect the performance of electronic components or cause high thermal stress. Therefore, there is an urgent need to develop thin, high-performance cooling devices that can achieve effective heat dissipation in confined spaces. Micro/nano-fabrication technologies offer solutions to address these challenges. Heat pipes, as efficient passive cooling devices, are widely used for heat dissipation in various electronic devices. High capillary pumping performance and heat transfer area capillary wicks can be obtained through micro/nano processing technology. This paper presents a comprehensive review on the types and applications of heat pipes and discusses the principles of enhancing heat transfer in heat pipes through micro/nano-structures. Furthermore, summarizes various fabrication methods for micro/nano-structured heat pipes, including chemical and oxidation treatment, laser processing, lithography technology and etching processes, electrical discharge machining, electrochemical deposition and so on. Finally, the characteristics of various fabrication methods together with the issues and challenges faced in the development of heat pipes are presented.

Key words: *Micro/nano-fabrication, electrodeposition process, laser machining, micro-heat pipes*

1. Introduction

The high integration and increased power of electronic devices have led to a dramatic increase in internal heat flux[1]. This increase in heat flux adversely affects the performance of electronic components, and the limited internal space makes it impossible to use traditional natural convection cooling methods for active cooling. To address the heat dissipation issues in electronic devices, the first approach is to use metals with high thermal conductivity, such as

copper, which has a thermal conductivity of approximately 400 W/(m·K). However, due to the inherent properties of metallic materials, their thermal conductivity cannot be significantly increased. With the advancement of thermal conductive materials, the high thermal conductivity of graphene has attracted significant attention. The thermal conductivity of single-layer graphene can reach up to 5000 W/(m·K)[2], and graphene-based materials, such as graphene films with high thermal conductivity and flexibility, can achieve a thermal conductivity of up to 1516.74 W/(m·K)[3], far exceeding that of copper. However, graphene must be used in relatively thin layers to achieve superior heat dissipation performance, which may not be ideal for heat dissipation in high-power electronic devices.

Heat pipes, as two-phase heat-transfer devices, can effectively lower the surface temperature of components by transferring heat from localized areas to larger cooling regions, thus achieving efficient thermal management[4]. The normal operation of a heat pipe relies on the internal capillary wick, which facilitates the liquid's return to the evaporation end through capillary pumping force, thus enabling the internal vapor-liquid circulation of the heat pipe. Common types of capillary wicks include: Copper mesh[5-8]; Spiral woven mesh[9, 10]; Microgrooves[11-14]; Porous copper foam[15-17]; Sintered copper powder[18-20]; Polymers[21-23] and so on.

An excellent capillary wick structure must possess high permeability and capillary force while maintaining low flow resistance to support the continuous evaporation-condensation cycle within the heat pipe. Copper mesh offers relatively high permeability but lower capillary force, whereas sintered copper powder exhibits higher capillary force but significant liquid flow resistance. To balance capillary force, permeability, and flow resistance, research on composite wick structures has been conducted, such as copper mesh combined with spiral woven mesh[24, 25], and microgroove combined with copper mesh[26, 27]. The small pores between the copper wires in the spiral woven mesh can serve as liquid flow channels while providing capillary force. Additionally, the spiral woven mesh can act as a support structure to prevent collapse during vacuum evacuation, and its proper arrangement can adjust internal vapor-liquid flow. Yan et al.[28] designed ultra-thin vapor chambers (UTVCs) with composite wicks structure composed of multi-layers copper mesh and spiral woven meshes. There are two types of the composite wicks: multi-layers copper mesh with a single spiral woven mesh and three spiral woven meshes. Under low heat load conditions, the UTVC with a composite wick containing a single spiral woven mesh exhibited lower thermal resistance and higher thermal conductivity. At higher heat loads, the UTVC with three spiral woven meshes demonstrated superior heat transfer performance, with a thermal conductivity of up to 11817.1 W/(m·K).

Additionally, high-performance biomimetic capillary wicks inspired by biological structures and their characteristics have garnered widespread attention. Wang et al.[29]inspired by the developed root systems of rice plants, created a biomimetic capillary wick composed of chemically treated copper fibers. The ultra-thin copper fiber wick (UTCFW) forms a micro-nano structure similar to root hairs on its surface and exhibits superhydrophilic properties after the chemical treatment. Experimental results indicated that the highly ordered fiber structure exhibits superior capillary performance. Zheng et al.[30]developed an asymmetric fractal grooved wick vapor chamber with a thickness of 1.2 mm, inspired by the pulmonary vascular network. Thermal testing of the vapor chamber was conducted using numerical simulations and

experimental methods, achieving a minimum thermal resistance of 0.23 K/W.

Some studies have developed wickless vapor chambers, where the internal working fluid transport relies on the design of surface wettability patterns. Damoulakis et al.[31]designed patterns with different geometric wettability, where the evaporation surface is capable of rapidly transporting condensed water to the heating area, and the condensation surface allows the condensed water to flow along specialized channels. Experimental testing achieved a minimum thermal resistance of 0.18 K/W. Luo et al.[32]designed a feather-shaped superhydrophobic-superhydrophilic pattern (SSP) for wickless vapor chambers. After hydrophobically treating the substrate, laser etching was used to process a superhydrophilic feather-shaped pattern onto the superhydrophobic surface. The optimized feather-shaped SSP achieved a maximum transportation velocity of 174 mm/s.

In recent years, significant research has been conducted on the development of ultra-thin, high-performance heat pipes. Micro-nano surface processing technologies have increasingly been applied to the treatment of wicks and condensation surfaces. Methods such as chemical oxidation[33], ion etching[34], and laser processing[35, 36] have been shown to effectively improve the wicking and heat transfer performance within heat pipes by creating micro-nano scale structures on the surface. This paper reviews various micro-nano processing methods used in heat pipes, building upon existing research in this area. Section 2 first introduces the various applications and types of heat pipes, including application of flexible heat pipe in electronic devices, lithium-ion battery thermal management system with vapor chamber and cold plate, a heating system coupled with solar flat heat pipe and phase change material unit and so on. Section 3.1 introduces the mechanisms of enhanced thin-film evaporation and boiling heat transfer through micro-nano structures, along with current efforts aimed at enhancing boiling heat transfer. Section 3.2 discusses the role of micro-nano structures in accelerating capillary flow and improving surface wettability. Section 3.3 summarizes research on enhancing condensation heat transfer, focusing on the control of droplet nucleation size and promotion of droplet removal through structured and mixed wettability surfaces. Section 4 presents various micro/nano processing techniques and the characteristics and properties of micro/nano structured capillary wick. Finally, the paper concludes with a discussion of the advantages and limitations of various micro-nano processing methods for heat pipes, and emphasizes the necessity of conducting experiments on enhanced boiling and condensation heat transfer under actual working conditions of heat pipes. Additionally, some suggestions are provided for the research on flexible heat pipes, particularly the exploration of materials with high thermal conductivity and mechanical strength for use in flexible heat pipe casings and wick structures.

2. Applications of heat pipes

Heat pipes have been widely used in various fields such as seawater desalination, heat dissipation of light-emitting diodes (LEDs), cooling of central processing units (CPUs), thermal management of permanent magnet synchronous motors (PMSMs), battery cooling, flexible electronics, solar energy collection and spacecraft thermal management due to their excellent thermal conductivity, as shown in Fig. 1. Flattened heat pipes, vapor chambers, loop heat pipes, flexible heat pipes, micro heat pipes and pulsating heat pipes are among the various types of

heat pipes that have been developed so far.

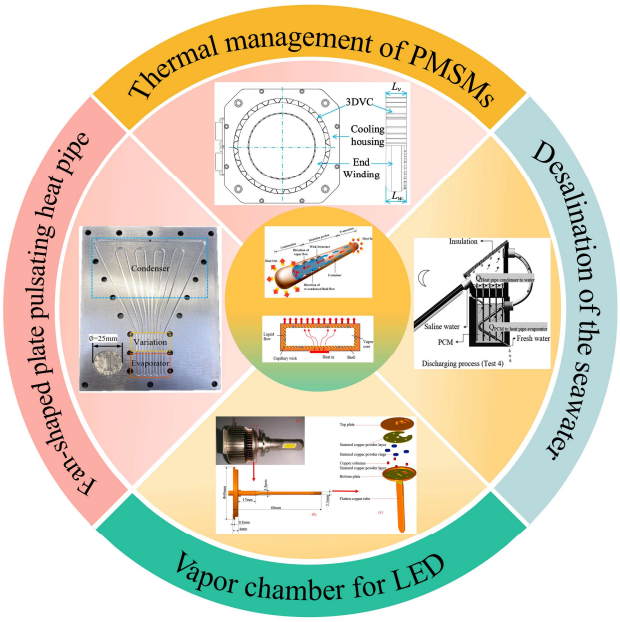

Fig. 1. Applications and types of heat pipes[37-41].

Cylindrical heat pipes can be transformed into flattened heat pipes using techniques such as phase-change flattening[42], cold roll forming, and lateral compression. Their shape can be modified to fit the thermal management space of electronic devices, with common configurations including three-dimensional bent shapes, flat-bent shapes, and linear shapes. Flattened heat pipes are primarily used in lightweight and portable electronic devices such as laptops, tablets, and smartphones. Zhou et al.[43]designed and fabricated ultra-thin flattened heat pipes (UTFHP) for smartphone cooling. The cooling module consisted of a copper plate and the ultra-thin flattened heat pipe. The experimental results indicated that the cooling module using the ultra-thin flattened heat pipe exhibited excellent temperature uniformity and higher maximum heat dissipation power compared to the module made with copper plates and sheets.

The rapid development and commercialization of foldable smartphones, flexible screens, wearable electronic devices, along with the efficient thermal management of the human body under extreme environmental conditions have accelerated the demand for the flexibility in the heat dissipation components in addition to high performance and ultra-thin characteristics. Sun et al.[44] inspired by the special structure of Microsorum fortunei leaf and designed the capillary wick structure consisting of sintered porous copper micropillars and multilayer copper mesh. They employed an alkaline oxidation method to deposit a layer of nanostructure on the surfaces of the copper wires and copper powder. The experimental results revealed that the biomimetic capillary core ultra-thin flexible heat pipe achieved a maximum thermal conductivity of 1943.5 W/(m·K), with a reduction in thermal conductivity of no more than 5.3% under bending conditions. Zhang et al.[45] inspired by the human spine, developed a novel biomimetic ultra-thin flexible heat pipe, using epoxy resin as the soft tissue material closely bonded to copper sheets. To ensure axial thermal conductivity of the tube shell, adjacent copper

sheets were connected by copper strips of a certain width. Under optimal filling conditions, the biomimetic flexible heat pipe with 3-layer copper mesh as the capillary wick achieved a maximum thermal conductivity of 1457.68 W/(m·K).

Solar energy is a renewable energy source, and utilizing photovoltaic and photothermal technology to convert solar energy into electrical and thermal energy plays a positive role in reducing fossil fuel usage and lowering carbon dioxide emissions. Phase change materials (PCMs) are widely used in solar thermal energy storage systems. However, the low thermal conductivity of PCMs limits the efficiency of these systems. Considering the high thermal conductivity of heat pipes, Wang et al.[46] combined flat plate heat pipes with phase change materials to establish an integrated building heating ceiling system using flat heat pipes (FHPs) and PCMs. The solar collectors' panels and FHPs effectively use the solar thermal energy and the heat storage function of the PCM helps reduce indoor temperature fluctuations. The system enabled efficient heat transfer into the indoor environment during the day and reduced heat exchange with the outdoor environment at night. The study explored the impact of heating power and the bending angle of FHPs on the integrated phase change thermal storage system.

The temperature of the CPU has a direct impact on the computing power of servers in data centers. The servers' computational speed and performance decrease as the CPU temperature rises. In practical applications, conventional liquid and air-cooling techniques have serious limitations. Loop heat pipes (LHP) have emerged as a promising cooling solution for data centers due to their long heat transfer distances, excellent thermal performance, and flexible layout. He et al.[47] fabricated a novel dual-evaporator ultra-thin LHP for cooling laptops, with a thickness of only 1 mm. The LHP utilized a sintered copper mesh as the capillary wick, which was arranged in a section of the liquid return circuit to serve as a water reservoir. Experimental results indicated that as the thermal load increased, the startup time gradually decreased. The minimum thermal resistance was 0.69 °C/W when the evaporator temperature was below 100 °C. Additionally, the maximum thermal load was higher when oriented in the direction of gravity compared to the horizontal orientation.

Lithium-ion batteries are widely used in electric vehicles due to their high energy density and long lifespan. However, Lithium-ion batteries are typically assembled into high-capacity battery modules, which generate substantial heat during the charging and discharging processes. If the heat is not effectively dissipated, its accumulation can adversely affect the battery's lifespan and even lead to thermal runaway issues. Cheng et al.[48] proposed a battery thermal management system that combines a VC and a minichannel cold plate. Compared to using a cold plate alone, the hybrid cooling mode improved the temperature uniformity of the battery module and exhibited the faster preheating capabilities in low-temperature environments. Among various renewable energy sources, hydrogen energy holds significant advantages due to its high energy density and environmental benefits. Proton exchange membrane fuel cells (PEMFCs) are one of the main methods for utilizing hydrogen energy. However, the conversion of chemical energy in the fuel to electrical energy generates substantial heat and if this heat is not dissipated on time, it can lead to temperature non-uniformity within the fuel cell, thus adversely affecting its performance. Zhao et al.[49] proposed a thermal management solution for PEMFCs based on a VC, integrating the vapor chamber into the PEMFCs design. The evaporation section is embedded inside the cell, while the condensation section is external,

allowing heat from the PEMFCs to be dissipated to the external environment. Thanks to the excellent thermal conductivity and isothermal characteristics of the VC, the internal temperature and temperature difference within the cell are significantly reduced. When the heat load is less than 40 W, the maximum temperature difference in the evaporation section is less than 4°C and in the condensation section is less than 1.5°C, respectively. In subsequent research[50], they investigated the thermal performance of PEMFCs integrated with vapor chambers under varying loads, cathode airflow rates, cooling airflow rates, load increments, and the effects of gravity.

In the aerospace field, the thermal management of electronic devices faces complex challenges due to environments such as microgravity or zero-gravity conditions, vacuum conditions, and strong vibrations during launch. Additionally, the radiation energy absorbed from the Sun or other celestial bodies can vary significantly while spacecraft are in orbit. Consequently, the thermal management technologies of electronic devices in spacecraft environments become highly challengeable. Although sintered capillary wicks exhibit strong capillary forces and excellent anti-gravity performance, they are produced by bonding through heating with the wall, making them susceptible to detachment in strong-vibration environments. As a result, spacecraft usually use more reliable groove wick heat pipes. Nesterov et al.[51] developed lightweight flat T-shaped titanium and copper heat pipes for thermal management of satellite electronic components, using acetonitrile and water as working fluids, respectively. The T-shaped design allows for efficient heat transfer between vertical surfaces. Experimental results showed that the flat copper heat pipe achieved higher heat dissipation power, while the flat T-shaped titanium heat pipe was significantly lighter and possessed greater strength.

3. Principle of the micro/nano structure enhanced heat transfer

The micro/nano structure in the heat pipes strengthen heat transfer can be analyzed from three aspects: Enhancement of heat transfer at the evaporation section, is primarily achieved by accelerating the vaporization of the working fluid. Enhancement of condensation heat transfer at the condensation end, the liquid drop is more readily nucleated and detached from the surface. Enhancement of capillary action, which speeds up the return flow of the condensed working fluid in the capillary wick, replenishing the working fluid lost due to vaporization at the evaporation section. Additionally, improving the surface wettability allows the liquid to fully wet the heating surface.

3.1. Enhancement of evaporation heat transfer

There are two modes of vaporization of the working fluid inside a heat pipe: evaporation and boiling. Evaporation primarily occurs on a micrometer-thick liquid film near the triple-phase contact line. The dense micro-nano structures on the surface of the capillary wick increase the area of the meniscus, thereby accelerating the evaporation rate[52]. When the thickness of the liquid film on the surface of the capillary wick exceeds a certain value, thin liquid film boiling occurs. At this point, both evaporation and boiling mechanisms are present within the vapor chamber of the heat pipe[53]. The occurrence of boiling enhances the heat transfer performance, and the boiling phenomenon is accompanied by the processes of bubble

nucleation, growth, and coalescence. Compared to flat surfaces, bubble nucleation is more likely to occur in small, narrow gaps. The liquid in these gaps is more significantly affected by heating than on flat surfaces, and gas is more likely to be retained in the gaps, with these gases serving as potential nucleation sites for vaporization. Micro-nano structured cavities on the surface of the capillary wick, created through micro-nano fabrication, can serve as potential nucleation sites for bubbles[54]. The size of nucleation sites ranges approximately from $2.54\times10^{-5}$to 2.54×10^{-7} meters. When calculating the boiling limit, the dimensions of micro-cavities are often considered as the critical nucleation size for bubbles[55]. Liu et al.[56] conducted a more in-depth study of bubble nucleation theory within the liquid film through reasonable assumptions and derived the critical thickness for bubble nucleation in the liquid film, as well as the maximum and minimum sizes of active micro-cavities and the minimum and maximum radius for bubble nucleation can be respectively determined as:

$$\delta_{f,c}=\frac{4\sigma T_v(1+\cos\theta)}{\rho_v h_{fg}(T_w-T_v)}\left(1+\sqrt{1+\frac{k_p T_w \rho_v \mathrm{h}_{fg}(T_w-T_v)}{2(1+\cos\theta)\sigma h_i T_v^2}}\right) \tag{1}$$

$$\{r_{c,\min},r_{c,\max}\}=\frac{\delta_f\sin\theta}{2(1+\cos\theta)}\times\left(1\mp\sqrt{1-\frac{8(1+\cos\theta)\sigma\left(k_p T_w+\delta_f h_i T_v\right)}{\rho_v \mathrm{h}_{fg} h_i\left(T_w-T_v\right)\delta_f^2}}\right) \tag{2}$$

$$\{r_{n,\min},r_{n,\max}\}=\frac{\delta_f}{2(1+\cos\theta)}\times\left(1\mp\sqrt{1-\frac{8(1+\cos\theta)\sigma\left(k_p T_w+\delta_f h_i T_v\right)}{\rho_v \mathrm{h}_{fg} h_i\left(T_w-T_v\right)\delta_f^2}}\right) \tag{3}$$

where θ being the contact angle, T_w is the temperature of the surface and T_v is the temperature of the bulk vapor, h_{fg} is the latent heat, δ_f is the liquid film thickness, σ is the surface tension, ρ_v is the density of the vapor, h_i is the heat transfer coefficient depending on vaporization at the liquid-vapor interface, k_p is the effective thermal conductivity.

In the process of liquid film boiling, bubble growth and coalescence form a gas film on the heated surface. The formation of this gas film hinders heat transfer between the solid surface and the liquid, leading to a sharp increase in temperature at the evaporation end. Effectively controlling the frequency and size of bubble detachment can significantly enhance heat transfer on the heating surface. Micro-nano scale structures can effectively reduce the detachment size of bubbles, increase the detachment frequency, and thus raise the critical heat flux of the heating surface. Related research has mainly focused on pool boiling experiments. The experimental results of Dong et al.[57] indicated that compared to smooth surfaces, micron-scale structures can effectively increase the density of active nucleation sites, while nano-scale structures can significantly reduce bubble detachment diameter and increase bubble departure frequency, thus delaying bubble coalescence into a vapor film. Wen et al.[58] prepared hierarchical nanowire structures with 1-10 μm micro-cavities between short nanowire clusters for bubble nucleation; microvalleys 35 μm deep between long nanowire arrays are designed to restrict bubble nucleation size and increase bubble departure frequency. Long et al.[59] used laser processing technology to prepare rose-petal-inspired hierarchical structures and micro-nano channels on a copper surface for bubble nucleation and liquid rewetting, respectively. The critical heat flux

and heat transfer coefficient were 2-fold and 4.6-fold higher than those on a smooth surface, respectively.

3.2. Enhancement of capillary pumping performance and improvement of surface wettability

After micro-nano fabrication, the numerous pores between the surface structures increase the capillary forces, accelerating the return flow of the liquid from the condenser end to the evaporator end. During nucleate boiling, the characteristics of the heated surface have a significant impact on the nucleate boiling phenomenon[60, 61]. As the heat flux increases, the frequency of bubble nucleation rises. During bubble growth, the area where the bubbles contact the heating surface can experience temperature increases due to a lack of liquid wettability. As the dry region at the bottom of the bubbles expands further, it may reach the critical heat flux (CHF)[62, 63]. Micro/nano-structures can accelerate the local increase in liquid wettability temperature, thereby delaying the occurrence of CHF. Wang[64] proposed a theoretical wicking model based on the effects of viscous forces and capillary forces of nano-structures on wicking speed and derived the diffusion coefficient of the liquid on the surface of nano-structures：

$$D = \frac{2\gamma h}{3\mu\beta}\frac{\cos\theta - \cos\theta_c}{\cos\theta_c} \tag{4}$$

where γ is the surface tension, h is the channel height, μ is the dynamic viscosity of the liquid, and β is the geometric parameter of the nano-structure.

During the flow of the liquid within the pores, the meniscus continuously changes, leading to variations in capillary forces with minimum and maximum values throughout the flow process. Alhosani et al.[65] studied the capillary forces driving liquid flow inside the modified mesh core and derived the following expression:

$$P_{\max} = \frac{2\sigma\cos\theta_{eq}(p+d)}{p^2 - pd} \tag{5}$$

$$P_{\min} = \frac{\sigma\cos\theta_{eq}\left(\frac{3p}{2}+d\right)}{p(p-d) - \frac{(p-d)d}{4}} \tag{6}$$

where σ represents the surface tension, p and d are parameters of the mesh core, and θ_{ep} is the equilibrium contact angle. For the modified mesh core, the contact angle $\theta_{ep} = 0$.

Chun et al.[66] fabricated a hierarchical nanowire structure containing interconnected V-Grooves, where densely uniform copper nanowires continuously provide capillary pressure. The V-shaped grooves between the nanowire clusters provide liquid flow channels and reduce viscous resistance. The study also investigated the effects of nanowire spacing, V-groove fraction, and groove depth on the wicking speed. Xie et al.[67]used ultrafast laser processing technology to fabricate gas-liquid partitioned micro-grooves on a copper surface. The micro-grooves consist of enhanced Laplace force structures and V-shaped structures. The enhanced

Laplace force micro-groove is characterized by a structure that is wider in the middle and narrower at the edges. When liquid flows in the micro-grooves, it generates capillary forces directed towards the central region. Based on the micro-groove structure, the expression for the capillary force was derived:

$$\Delta P_2 - \Delta P_1 = \frac{4\gamma\cos\theta}{\alpha}\left(\frac{1}{x_2} - \frac{1}{x_1 + x_2}\right) + 2\gamma\sin\theta\left(\frac{1}{x_2} + \frac{1}{x_1 + x_2}\right) \tag{7}$$

where γ represents the surface tension, θ is the contact angle, and x_1, x_2, and α are as shown in Fig. 2.

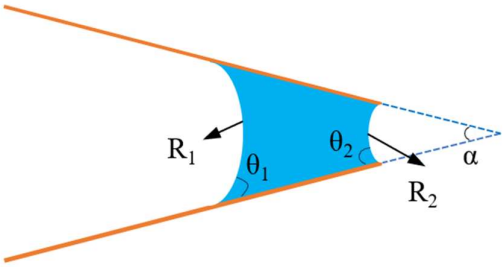

Fig. 2. Enhanced Laplace force structures.

Wu et al.[68] used laser processing to fabricate micro-groove structures and produced nanometer-scale ripples inside the micro-grooves through secondary ablation and polishing. The model previously used to predict the variation in wicking height had significant errors. By introducing a correction factor, which depends on the changes in surface energy caused by the nanostructures, the enhancement of wicking was quantitatively characterized. The prediction error of the improved model is reduced from 72.9% to 4.5%.

$$h^2 = \frac{2\sigma}{\mu k_\mu}(\lambda S\cos\theta - w)\cdot t \quad k_\mu = \frac{\Delta p}{\mu L}\cdot\frac{A^2}{Q} \tag{8}$$

where λ is the correction factor and is greater than 1, S is the cross-sectional area of the groove or the perimeter of the wetted area, w is the length of the liquid contour, A is the cross-sectional area of the groove, and Q is the flow rate.

3.3. Enhancement of condensation heat transfer

Condensation typically occurs in two modes: filmwise condensation (FWC) and dropwise condensation (DWC). In filmwise condensation, a liquid film forms on the condenser surface, which increases the thermal resistance between the vapor-liquid and the cold wall. In contrast, dropwise condensation on a hydrophobic surface result in the nucleation, growth, and coalescence of discrete, larger droplets that eventually detach. This mode of condensation has a stronger heat transfer effect compared to filmwise condensation[69]. Wettable surfaces, on the other hand, more readily form droplets[70], but these droplets are difficult to remove. To

enhance condensation heat transfer, the condenser surface can be processed to create a superhydrophobic surface. Three distinct wetting states may exist on the condensation surface: the Cassie state, where liquid droplets suspend on the surface of micro/nanostructures; the Wenzel state, where liquid droplets immerse the surface of micro/nano-structures; Another kind is in a transitional state between the Cassie and Wenzel states, where the droplet partially immerses the surface of micro/nano-structures[71].To ensure effective droplet detachment, droplets should ideally remain in the suspended or partially wetted Cassie state[72]. As the wall supercooling increases, droplets transition from the suspended state to the wetted state, making it difficult to remove them[73], and wetted droplets can coalesce to form a liquid film, reducing the heat transfer capacity.

Condensation begins with initially small clusters. When the size of these clusters exceeds the critical size determined by the contributions of the interfacial and volumetric Gibbs free energy, these microscopic units further grow to form the liquid phase. The critical nucleation radius of droplets can be obtained from the Kelvin equation:

$$r_e = \frac{2T_v\sigma_{lv}}{h_{fg}\rho_l\Delta T} \tag{9}$$

where Tv represents the vapor temperature, h_{fg} is the latent heat, σ_{lv} is the liquid-vapor surface tension, ΔT is the supercooling, and ρ_l is the liquid density. From the equation, it can be observed that as the supercooling increases, the critical nucleation radius continually decreases. The critical nucleation size of droplets can reduce from several nanometers at low supercooling to approximately 1 nm at high supercooling[74].

Optimizing surface structures to control the size of droplets during detachment and to accelerate the frequency of droplet removal can enhance condensation heat transfer. Wen et al.[75] utilized the spatial effects of nanowires to prevent vapor molecules from entering the nanowires in large quantities, thereby enhancing heat transfer by forming droplets on the nanowire surface. Gao et al.[76]designed superhydrophobic micro-channel structures (using superhydrophobic nano-coatings) to accelerate droplet removal. The primary channels remove small-sized droplets, while the secondary channels remove larger droplets. However, the nucleation and removal of condensation droplets have different requirements for surface properties[77]. Hydrophilic surfaces with high surface energy can effectively lower the nucleation energy barrier, facilitating droplet nucleation, while hydrophobic surfaces with low surface energy can reduce surface adhesion, promoting rapid droplet detachment. Therefore, Tang et al.[78] and Zhou et al.[79] combined superhydrophobic and hydrophilic surfaces to achieve rapid nucleation and removal of droplets. Wen et al.[80] combined the characteristics of filmwise and dropwise condensation by fabricating a superhydrophobic hierarchical mesh-covered surface to enable continuous sucking flow of condensed liquid. The experiment was carried out at the water vapor pressure of 60kPa (approximate to heat pipe vacuum conditions), observed condensation heat transfer enhancement and three types of droplet jumping: self-jumping induced by droplets coalescence on the copper mesh wires, self-jumping of a single droplet in micropores, and mixed jumping of droplets both inside and outside micropores.

Given the role of superhydrophilic, superhydrophobic, and hybrid wetting surfaces in

enhancing boiling and condensation heat transfer, structured surfaces that promote droplet jumping, increase bubble generation and detachment, reduce flow resistance will become an up-and-coming choice for capillary wick design of heat pipes. The manufacturing of superhydrophobic surfaces relies on the use of superhydrophobic coatings, however, ensuring the long-term stability of superhydrophobic coatings under the action of vapor pressure inside heat pipes still requires further research.

4. Fabrication of micro/nano structured surface

The methods for fabricating micro/nano structured surfaces include chemical oxidation, laser processing (where high-temperature oxidation occurs during laser processing), ion etching, anodic aluminum oxide (AAO) template-assisted oxidation, and nanoparticle deposition. Chemical oxidation and AAO template-assisted oxidation can be used to fabricate nanostructures such as nanograsses, nanosheets and nanowires. Laser processing, etching techniques, and electrical discharge machining (EDM) can be used to create microgrooves, micropillars, and other microstructures. The following will explore the process flow, surface morphology characteristics of micro/nano structures, and pumping performance of capillary structures using different processing methods.

4.1. Chemical and oxidation treatment

There has been extensive research on fabricating micro-nano structures on capillary wick surfaces using chemical oxidation methods. Compared to untreated capillary wicks, oxidized wicks exhibit enhanced hydrophilicity. Common oxidation methods include alkaline oxidation and thermal oxidation. Prior to oxidation, pretreatment is typically performed to remove surface impurities and oxide layers. The pretreatment process generally involves sequential ultrasonic cleaning of the capillary wick in acetone, isopropanol, anhydrous ethanol, and deionized water. The cleaned copper mesh is then soaked in pre-diluted hydrochloric acid for to remove the surface oxide protective layer. Wu et al.[81] immersed the pretreated copper mesh in a 1 mol/L oxalic acid solution at a temperature of 80°C. After a period reaction time, the mesh was washed with anhydrous ethanol and water, then dried in a vacuum drying oven. This process created a multiscale structure on the copper mesh surface, including nanosheets, as shown in Fig. 3(a). When the treatment time was 22 h, the capillary rise height of the capillary wick reached 91 mm, with a capillary rise rate of 8.4 mm/s. Wen et al.[53, 82] stacked copper meshes with copper plates and tightened them with stainless steel flanges in a vacuum oven for 4 hours, resulting in bonding between the mesh and plates. Subsequently, the bonded mesh was treated in an alkaline solution to obtain mesh wicking structures with nanograsses. A chemical cleaning process was then used to remove the nanograsses, and micro-cavities were created on the mesh and substrate surfaces. Huang et al.[24] placed sintered composite capillary wicks in a sintering furnace connected to external air. The temperature was raised at 8°C/min to 400°C, 500°C, 600°C, and 700°C, holding each temperature for 150 minutes before cooling to room temperature. This produced micro-nano structures of Cu_2O or CuO on the capillary wick surface (limiting working fluid selection). The oxidized capillary wicks were then subjected to reduction treatment in the furnace, and cooled to room temperature. Reduction gas was passed

into the furnace during the heating and cooling process. Li[83] soaked the capillary wick in hydrogen peroxide for 8 hours, and then dried it in an oven to obtain a superhydrophilic capillary wick.

The heat transfer limit of a thermal spreader is constrained by the internal working fluid circulation. Improving the internal fluid circulation can enhance the heat transfer performance of the spreader. To promote the working fluid circulation, strategies include increasing the capillary forces to enhance the fluid reflux within the wick and accelerating the detachment of the condensed liquid from the condensation surface. Inducing droplet coalescence and jumping on the condensation surface can effectively facilitate the working fluid's return to the evaporator. To speed up droplet detachment, the condensation surface is often treated to be superhydrophobic. Recent research on Jumping Droplet Vapor Chambers (JDVCs) has explored this approach. Wei et al.[84] developed a VC combining superhydrophobic and superhydrophilic structured surfaces. They sintered a copper mesh onto the condenser surface and treated it with the same method as Sun et al. [85] to achieve a superhydrophobic surface. The evaporator wick used gradient-pore-size sintered copper foam, which was chemically treated to produce a superhydrophilic CuO composite microstructure, and including multi-scale channels that enhance liquid flow. The study experimentally tested the effects of condenser mesh pore size, the number of microchannels in the evaporator wick, and radial and axial gradients on the thermal performance of the VC.

Fabricating micro/nano structures on copper mesh surfaces is a common method to enhance the wettability of the copper mesh. However, structures such as nanosheets and nanograsses may not maintain long-term reliability under high temperatures and fluid conditions. Thus, it is essential to develop new micro/nano fabrication techniques to improve the stability of these nano-structures. Li et al.[86] transferred the pre-treated copper mesh to a vacuum sintering furnace, slowly increasing the temperature to 500°C over two hours, holding for 30 minutes, and then raising it to 850°C within an hour, holding for 30 minutes, and cooling slowly to room temperature. The sintering process was conducted under nitrogen protection, resulting in nanometer-sized grooves on the copper wire surface, as shown in Fig. 3(b).

Foamed metals, with their exceptionally high porosity and surface area, have emerged as key materials for high-performance capillary wicks. The capillary pumping performance and heat transfer properties of foamed metal capillary wicks can be further improved by fabricating nano-structures on their surfaces through chemical treatments. Shum et al.[87] used a blackening process to create superhydrophilic oxides on foam copper surfaces. The cleaned foam copper was subjected to acid treatment in a stirrer at 250 rpm for 1 hour. After deionized water cleaning, it was dried in a vacuum oven at 70°C and 20 psi for 20 minutes. The foam copper was then placed into a stirrer with a solution of NaOH (2M) and $NaClO_2$ (2M), followed by final cleaning. The experimental results showed that the treated metal foams achieved a wicking height of 140mm compared to no treatment. Sun et al.[88] used foam nickel as the capillary wick. The cleaned and dried foam nickel was immersed in hot alkaline solution to produce various nanostructures by controlling oxidation temperature and time, as shown in Fig. 3(c). According to research, the permeability increased with a maximum enhancement of 34.7% and the effective capillary radius decreased with a maximum reduction of 14.9% as the degree of oxidation increases. These studies demonstrate various methods for preparing micro-nano

structures on capillary wicks, significantly enhancing their properties, such as hydrophilicity and capillary pumping performance.

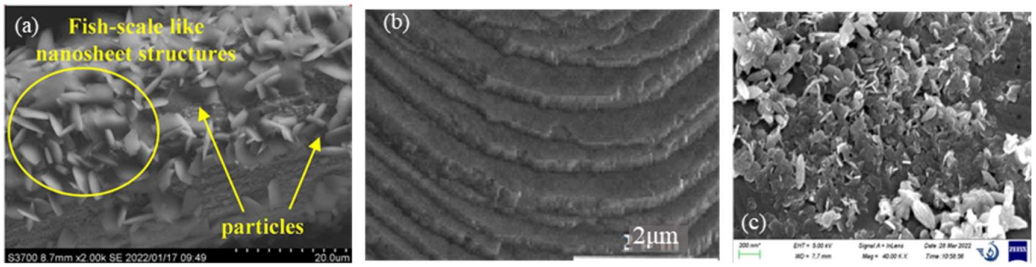

Fig. 3. (a) SEM image of nanosheets and particles, (b) SEM image of the nanometer-scale microgrooves [86], (c) nanometer-scale particles on the surface of foam nickel[88].

4.2. Laser processing technology

Ultrafast laser processing technology can fabricate complex micro-nano structures for capillary wicks. During the laser ablation process, the material surface oxidizes at high temperatures, resulting in nano-structures[89] and micro-cavities, which improve surface wettability[90] and increase nucleation sites. Simultaneously, the high energy density at the laser center results in a V-shaped cross-sectional profile for the micro-grooves produced. In recent years, extensive research has been conducted in this area. Long[35] used nanosecond laser processing to fabricate dual-scale porous structures and microgrooves on copper substrates, and conducted capillary pumping performance experiments. Results indicated that micro-grooves had a high capillary rise velocity compared to porous structures. Porous structures had numerous nanometer-sized particles distributed on their surfaces, which enhanced capillary forces but also increased flow resistance. Based on the characteristics of the two structures, porous structures were used for the condenser and micro-groove structures for the evaporator to prepare a VC. Liu et al.[91] conducted laser etching on copper mesh wicks. The surface of the bare copper mesh is relatively smooth, but after laser etching, the surface roughness of the copper mesh significantly increased, and micro-cavities were formed on the surface. These micro-cavities provide nucleation sites for film boiling and increase the heat transfer area, and the treated mesh wick exhibits superhydrophilicity. Additionally studied was the impact of the etched area on the VC's thermal performance. Yuan[92] utilized nanosecond laser processing to fabricate a multi-scale microgroove wick (MSMGW) for ultrathin ceramic heat pipes. The MSMGW has a thickness of only 66 μm, and the ceramic materials used include alumina, aluminum nitride, and silicon carbide. The effects of laser scan spacing, speed, power, and repetition frequency on the capillary pumping performance of the wicks were investigated. Under optimal configuration parameters, the experimental results indicated that the capillary rise height of the MSMGW reached 114 mm within 28 seconds, and the capillary performance parameter (K/Reff) was 1.49 μm.

Biomimicry has provided new ideas for the design of capillary wicks, and combining laser processing with biomimetic concepts can produce high-performance capillary wicks. Some researchers have explored biomimetic microgroove wicks inspired by plants and animals. Jiang et al.[93] used a picosecond laser to develop a dual-height microgroove wick (DHMW) inspired

by a pitcher plant on aluminum alloy. The dual-height microgrooves consist of high ribs and minor ribs, creating primary liquid flow channels between adjacent high ribs and smaller channels between minor ribs, as shown in Fig. 4. Compared to normal microgrooves (NM), the dual-height microgrooves (high rib height: 236.7 μm, minor rib height: 205.1 μm) achieved a capillary performance parameter (K/Reff) of 1.182 μm, and an average wicking rate of 14.566 mm/s, representing increases of 71.3% and 16.5%, respectively.

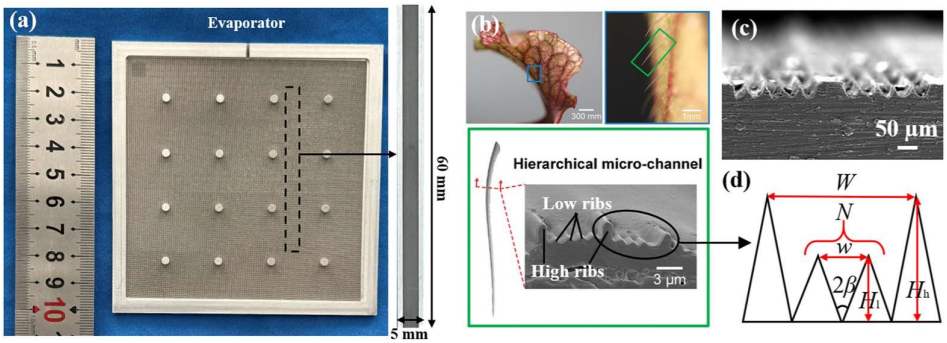

Fig. 4. Image of the evaporator wick and SEM image of the DHMW[93].

Laser processing can be used to create structures with specific functionalities by adjusting laser processing parameters to fabricate microgrooves that modulate the liquid-vapor flow characteristics within a heat pipe. Xie et al.[67] used ultrafast laser processing technology to create gas-liquid partitioned microgroove wicks composed of V-shaped grooves and enhanced Laplace force structures. The Laplace pressure caused by the variation of microgroove width during liquid flow in the groove can promote liquid flow. Jiang et al.[13] controlled laser scanning intervals, speeds, and modes to fabricate a three-zone hybrid structure on a substrate surface. This structure comprises an evaporation zone, a water/vapor transport zone and a condensation water reflux zone. And cross-arrayed micro-protrusions (CMPs) and parallel micro-channels (PMCs) were fabricated on the evaporation, condensation regions and the water/vapor transport zone, respectively. According to capillary rise and evaporation experiments, the PMCs exhibited the great antigravity-wicking performance and high-speed water delivery capability; compared to the PMCs, the CMPs had the higher evaporation rate.

Aluminum and titanium alloys are widely used in lightweight two-phase heat exchangers due to their excellent corrosion resistance and low density. High performance and lightweight heat pipes can be prepared using laser processing technology with aluminum alloy and titanium alloy as substrates. Wu et al.[68] used a multi-beam laser parallel processing method to fabricate ultra-thin microgrooves titanium wick with varying aspect ratios and superhydrophilic nano ripples. The capillary performance of the micro/nano-structured wicks was studied. Optimizing microgroove wicks using an improved wicking dynamics model, achieving a maximum capillary performance parameter of 1.8 μm at a thickness of 80 μm. This represents a 56.7% improvement over traditional V-shaped grooves. Besides, the critical heat flux of 15 W/cm² with a device size of 30 mm × 100 mm. Lou et al.[94] utilized a laser etching-sputtering technique to fabricate dual-shape hybrid grooves (DSHG) on aluminum sheet, as shown in Fig. 15. During the laser etching process to create tapered grooves, continuous laser impact was used to melt the material. The high-energy laser caused sputtering of the molten material, and

the sputtered micro/nanoparticles solidified and accumulated at the edges of the tapered grooves, then formed secondary rectangular grooves. In capillary rise tests, the rise rate for the first 2 seconds was 24 mm/s, and the height reached 200 mm in 85 seconds. Compared to tapered grooves, the DSHG showed a 22.5% increase in rise height within 85 seconds.

Due to the computer-controlled parameters and motion paths in laser processing, laser machining offers high efficiency and repeatability. Typical laser processing methods include nanosecond, femtosecond, and picosecond machining. Thermal diffusion in the processing area is reduced by narrowing the pulse width. The short material-laser interaction time, especially in picosecond and femtosecond machining, allows for the creation of intricate, superior surfaces. Moreover, laser processing can be utilized to create microstructures on polymer films. The high processing temperatures carbonize the polymer, increasing surface wettability and greatly boosting the polymer film's capacity for heat transmission. It is possible to use this technology to create flexible heat pipes.

4.3. Etching process and electrical discharge machining

Etching processes are utilized for fabricating smaller-scale grooves and are widely applied in micro/nanofabrication. Etching can be classified into dry etching and wet etching based on the processing technique. Dry etching offers advantages including quick etching speed, good anisotropy, low etching damage, and a smooth etching surface, but it also has significant equipment requirements when processing in a vacuum environment. It has considerable advantages in the processing of materials such as silicon, organic compounds, and metals. Wet etching involves the use of chemical reagents to corrode the material under the protection of a photoresist layer, and after cleaning and removing the photoresist, the desired pattern is obtained. This method is characterized by its simplicity, selective corrosion, and isotropy. However, it is not suitable for fabricating patterns smaller than 3 μm, and during processing, bubbles may form, hindering corrosion in the areas where they adhere[95]. Kang et al.[96] utilized the wet etching process to fabricate micro heat pipes (MHPs) with star and rhombus grooves. The star grooves were created by wet etching a series of V-shaped channels on three silicon wafers, which were then bonded together using eutectic bonding technology. The rhombus grooves MHP was produced using the same technique on two silicon wafers. Chen et al.[97] also used wet etching to fabricate vapor and liquid channels on a copper substrate. The top plate, bottom plate, and capillary wick were then bonded together through diffusion welding. The top plate featured micro-pillars of varying densities and sizes, while copper mesh is placed in micro grooves on the bottom plate with an etching depth of 0.08 mm, and the resulting UTVC is only 0.4 mm thick.

Zhao et al.[98] developed a biomimetic electrospray vapor chamber (BEVAC). The BEVAC had a beetle-inspired the superhydrophobic-hydrophilic condensation surface fabricated by reactive ion etching (RIE). The top of the surface has hydrophilic bumps, whereas the surface is superhydrophobic throughout. When the BEVAC was working, the working fluid vaporized from the evaporator and condensed on the hydrophilic bumps and then the liquid return was enabled by electrospraying from the condenser to evaporator. Liu et al.[99] designed a biomimetic vapor chamber inspired by leaf-vein-like fractal network and micro fin-pins. The

leaf-vein-like condenser wick was fabricated by etching processes, while the evaporator wick was made from sintered copper powder. Experimental tests revealed that the VC exhibited optimal thermal performance when the fractal angle ranged between 40° and 50°. Specifically, a fractal angle of 45° achieved a thermal resistance of approximately 0.06°C/W when the condenser wick was fabricated using the etching process. Lv et al.[100] initially coated a silicon wafer with a photoresist layer and used ultraviolet lithography with a reverse mask to transfer the desired pattern onto the wafer. Subsequently, an aluminum film was sputtered on the wafer surface using a magnetron sputtering technique. After cleaning and drying the wafer, the deep plasma etching process was used to process micro-grooves on the silicon wafer. The heat pipe was then assembled by vacuum anodic bonding.

Etching process has the characteristics of high processing accuracy, small size, and controllable structure, and can be used to fabricate micron-scale grooved wicks. Although etching technology has great advantages in micro heat pipe processing, the process needs to be combined with photolithography technology, resulting in high processing costs. In the future, it is necessary to optimize the processing flow and improve the processing technology to reduce production costs.

Electrical discharge machining (EDM) is a non-contact processing method that utilizes a tool electrode to fabricate high-aspect-ratio microgrooves on conductive substrates. During the machining process, molten metal deposits onto the microgroove structures, forming micro-nanostructures, which enhance capillary performance and surface heat transfer[101]. Nishida et al.[102] employed EDM to produce three types of microgroove heat pipes. The widths and depths of the three types of microgrooves were 35 μm and 30 μm, 35 μm and 48 μm, and 35 μm and 30 μm, respectively. Experimental results showed that the heat pipe with microgrooves measuring 35 μm in width and 30 μm in depth exhibited superior performance. Zhou et al.[103] fabricated a cylindrical micro heat pipe (MHP) using wire electrical discharge machining (WEDM). The width and depth of the microgrooves were approximately 170 μm and 220 μm, respectively. Experimental results indicated that under a heat load of 150 mW, the heat pipe using the nanofluid with a mass concentration of 0.5 wt% as the working fluid achieved a minimum thermal resistance of 0.33°C/W. Tang et al.[104] utilized WEDM and electrical discharge machining shaping(EDMS) techniques to fabricate interconnected microgroove arrays and microstructures on a substrate surface, as shown in Fig. 5. Initially, WEDM was used to create microgrooves, which were divided into three secondary microgrooves each by two micro fins. Subsequently, the workpiece was rotated 90° and EDMS was used to produce a wavy pattern. Capillary rise experiments were conducted using ethanol as the working fluid，the capillary height and the capillary parameter（K/R_{eff}）reached 60.4mm and 1.57μm, respectively.

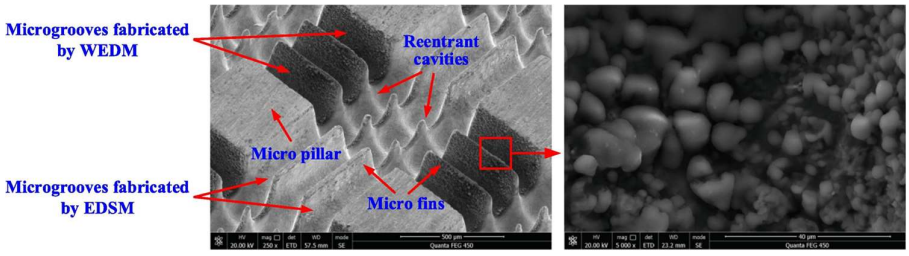

Fig. 5. SEM image of wick structure fabricated by the combination of WEDM and EDSM[104].

4.4. Micro/nano structures fabricated by other machining methods

In addition to the above processing methods, coating technology can also be used to modify the surface of the substrate. Currently, commonly used coating materials include SiO_2, TiO_2, carbon nanotubes (CNTs) or other nanoparticles. Common coating methods include atomic layer deposition, chemical vapor deposition, electrochemical deposition, etc. The following section reviews the research progress in the preparation of micro/nano structures using coating technology and hybrid processing methods.

4.4.1 Surface coating technology

Using nanofluids as working fluids in nucleate boiling studies can have significant effects on the system's heat transfer properties. Using nanofluids improves the surface characteristics by forming a coating of nanoparticles on the heated surface. This nanoparticle layer facilitates the flowing of liquid into the heating surface through capillary action, which delays dryout and substantially increases the critical heat flux[105, 106].

Ghanbarpour et al.[107] investigated the heat transfer characteristics of heat pipes using water-based Al_2O_3 nanofluids. The study revealed that heat pipes using Al_2O_3 nanofluids with a 5 wt.% concentration maintained nearly consistent wall temperatures in the evaporation section during increases and decreases in thermal load. For heat pipes using deionized water as the working fluid, during the process of reducing heat load, the wall temperature of the evaporation section is higher than that when the heat load increases. This discrepancy arises because the nanoparticle layer formed during heating in nanofluid-based heat pipes alters surface wettability, roughness, and nucleation site density, while suspended nanoparticles impact bubble dynamics[108]. Gupta et al.[109] applied physical vapor deposition to coat TiO_2 nanoparticles on capillary wicks, achieving an average pore size of 2-4 μm and a thickness of 400 nm. Physical vapor deposition offers controllable coating thickness with low cost, minimal contamination and fast processing. Experimental results showed that heat pipes with capillary wick coatings had thermal performance similar to that of heat pipes using nanofluids and nanoparticle coatings could replace nanofluids.

For complex-shaped components and flexible electronic devices, using metal meshes as capillary wicks may adversely affect heat pipe performance due to limited metal ductility. Polymers, with their flexibility and lightweight properties, are considered as potential capillary wick materials. However, polymers have significantly lower thermal conductivity compared to metals, prompting extensive research to improve polymer thermal conductivity. Methods such as chemical vapor deposition (CVD)[110], surface-initiated polymerization[111], atomic layer deposition (ALD)[112], sol-gel processes[113], and ultrafast laser texturing[114] have been explored to enhance polymer thermal conductivity and improve wettability. Lewis et al.[22] utilized polyimide (Kapton) as the shell material and SU-8 for the liquid wicking structure and pillars to support the casing. To provide the surface moisture barrier and hydrophilicity, a TiO_2 film was deposited on the SU-8 and Kapton surfaces via ALD. This process resulted in a ultra-

thin all-polymer flexible thermal ground plane (FTGP) with a thickness of only 0.3 mm. Tang et al.[115] developed novel superhydrophilic nylon mesh wicks (SNMWs) for enhancing the thermal performance and bending reliability of flexible heat pipes (FHPs). The sol-gel method was used to modify the nylon mesh to achieve superhydrophilicity. After the treatment, the surface of SNMWs displayed nanoparticles, microwrinkles, and cracks, all of which enhanced its hydrophilicity. The experimental results showed that compared to untreated NMWs, the maximum wicking coefficient of the SNMWs reached 5.91mm/$s^{0.5}$, and the equilibrated wicking height increased by 695.7%.

Electrochemical deposition can be used to fabricate high-surface-area porous structures. By controlling the amount of electrical current, various morphologies of deposits, such as "dendritic" or "honeycomb" structures can be achieved[116]. Additionally, it can be employed to create porous structures on the sidewalls or support columns within vapor chambers to enhance the circulation of the internal working fluid. The numerous micropores in the deposited material can serve as nucleation sites for bubbles, increasing bubble formation and thus facilitating boiling heat transfer. Wen et al.[58, 74, 75, 117] have conducted extensive research on enhancing boiling and condensation heat transfer using nanowires. Nanowires were prepared using a two-step process porous anodic aluminum (PAA) oxide template-assisted electro-deposition method. And copper micro pillars are created on the copper surface through photolithography and wet etching, followed by electrodeposition. Due to the different growth times of nanowires on the micro pillars, longer nanowires are formed at the top of the micro pillars, while shorter nanowires are formed in the gaps between the micro pillars, resulting in a layered nanowire structure. Fig. 6 shows the hierarchical nanowire arrays and wettability. A slightly lower purity aluminum oxide template was used for fabricating the three-dimensional nanowire structure. Because of the nanoscale side holes in this template, after electrodeposition the nanowire surfaces developed interconnected protrusions, which prevented the formation of micro-defects between nanowire clusters. Luo et al.[118] used electrochemical deposition to fabricate biomimetic copper forest wick. Various deposition morphologies were obtained by varying the electrodeposition duration and current amplitude respectively. During the electrodeposition, adjacent dendrites formed Ω-shaped microgrooves to provide flow space for the working fluid. With increased deposition time, the height and branching of the deposits increased, ultimately the wick had a high porosity rate that could reach up to 80%. Yu et al.[119] used electrochemical deposition to prepare micron-sized dendritic copper wicks on the surface of copper. By varying the electrodeposition current density and electrolyte concentration, copper wicks with various porosity characteristics can be prepared. To enhance the capillary performance, adhesion, and structural integrity of the deposited copper wick, the copper wick was thermally treated in a nitrogen environment at 700°C for 90 minutes. After heat treatment, the porosity of the thick copper wick reached 0.936, and the capillary performance parameter K/R_{eff} achieved 1.5 μm.

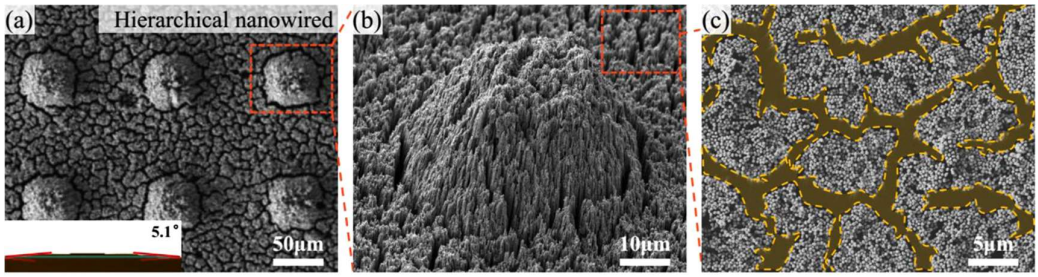

Fig. 6. SEM images of the two-level hierarchical surface and wettability of the different surfaces[58].

CNTs are used in wick structures due to their high surface area, low density, and nanoscale network characteristics. CNTs are cylindrical structures composed of graphitic carbon. A typical CNT array consists of CNTs with average lengths of between 50 nm and 1 mm and average diameters ranging from 10 to 500 nm. The average spacing between CNTs is about 3 to 8 times their diameter[120]. The nanoscale pores within the CNT arrays provide capillary forces that facilitate liquid flow. However, the hydrophobic nature of CNTs limits their application, necessitating the use of surface functionalization techniques to improve their wettability. Cai et al.[121, 122] fabricated a CNT biwick using micro-electromechanical systems (MEMS) technology on a silicon substrate. The CNTs on the substrate were primarily produced through a thermal CVD method. The CNTs were hydrophilic after being treated with acid to change surface wettability. The nanoscale gaps within the CNT clusters formed the primary capillary structure, while the spacing between the clusters formed the secondary capillary structure. Experimental testing showed that the biwick could achieve a heat flux of 700 W/cm² in a 2 mm × 2 mm heating area. Kousalya et al.[123] fabricated CNTs on 200 μm thick sintered copper powder using microwave plasma chemical vapor deposition (MPCVD). To enhance the wettability of the CNT structure, they subsequently coated the CNT surface with copper of varying thicknesses through physical vapor deposition (PVD). Experimental tests showed that a sample with a deposition layer thickness of 750 nm exhibited an equilibrium contact angle of 35°. In a 5 mm × 5 mm heat input area, the CNT-coated samples could support a dryout heat flux of 457 W/cm². Lee et al.[124] designed and fabricated a biporous wick heat pipe using a layer-by-layer (LBL) deposition method. The fibrous multi-walled carbon nanotube (MWCNT) network exhibited a biporous structure, and the hydrophilic polyethyleneimine (PEI) coating improved the wettability of the biporous wick. The intrinsic contact angle of CNT was 167±3°. Experimental results showed that the static contact angle of MWCNT with a PEI coating could be reduced to 51.8°. Additionally, a heat pipe with MWCNT-PEI coating in 10 bilayers exhibited lower thermal resistance and a higher heat transfer coefficient.

4.4.2 Hybrid processing methods

By leveraging the advantages of composite wick structures, hybrid processing methods can produce structures that combine high heat transfer performance with efficient capillary pumping capabilities. Hybrid processing primarily focuses on improving surface wettability, increasing heat transfer area, reducing fluid flow resistance, and enhancing capillary action.

Chen et al.[125] utilized anodized aluminum oxide-assisted electrodeposition and WEDM technology to fabricate a composite structure of nanowires and microgrooves, which increased nucleation site density and strengthened capillary action. The study investigated the effects of nanowire height and microgroove spacing on the boiling heat transfer performance of the composite structure. The optimal pool boiling critical heat flux (CHF) was achieved on a nanowire-microgroove surface with a nanowire height of 25 μm and a microgroove spacing of 0.5 mm. Lu et al.[126] employed a combination of planing, electrochemical deposition, and heat treatment to fabricate a composite wick structure that combines a porous deposition layer with rectangular microgrooves on the surface of a copper plate. After planing and coating the surface of the copper plate with a protective layer , and an untreated copper plate was used as the anode and a treated copper plate as the cathode for electrochemical deposition. The capillary wick samples were then subjected to heat treatment to improve their wettability. Sudhan et al.[127] initially used EDM to form axial grooves at the inner wall of an aluminum tube and then carried out the anodization technique to make an porous coating at the inner surface of the heat pipe. The presence of the porous layer further enhanced the capillary force. At lower heat load inputs, the anodized grooved heat pipe with a groove width of 0.4 mm had a thermal resistance that was 70% lower than that of the non-anodized grooved heat pipe. Li et al.[128] developed grooved nanocarbon foams (GNCFs) based on carbon nanotubes as capillary wicks for heat pipes, as shown in Fig. 7(b). The NCFs feature a biporous structure comprising micro-scale pores within the CNT networks and nano-scale pores within the CNTs themselves. The NCFs were fabricated using a template method and the micro-grooves were prepared through laser cutting process. Experimental tests showed that GNCFs with eight grooves, achieved a maximum capillary rise height of 45 mm within 14 seconds. He et al.[129] utilized the roller pressing process in conjunction with laser processing technology to fabricate a hierarchical Ω-shaped aluminum micro-grooves capillary wick, as shown in Fig. 7(c). The laser-processed layered micro-groove structure increased the capillary radius on the aluminum micro-grooves wick surface and enhanced its surface anisotropy, causing the liquid on the surface to preferentially extend parallel to the grooves. Under the optimal laser processing parameters, the fabricated hierarchical micro-grooves wick achieved a maximum capillary rise height of 88.5 mm.

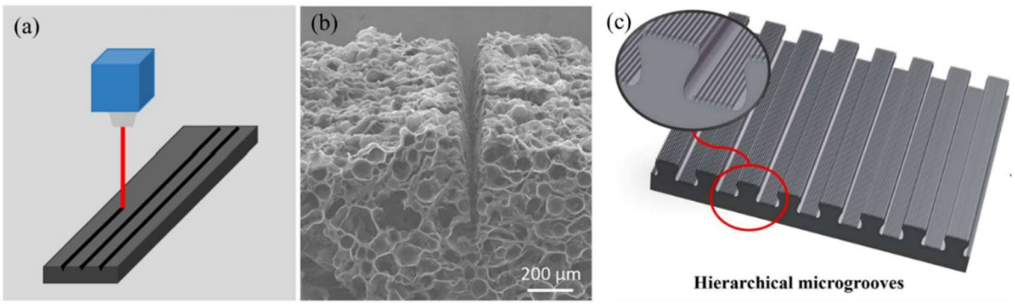

Fig. 7. (a) Schematic of the microgrooves fabrication and (b) SEM image of the GNCF[128], (c)Schematic of the hierarchical microgrooves[129].

The above summarizes methods for fabricating micro-nanostructures on heat pipe capillary wicks or substrate surfaces. Table 1 provides parameters and performance details for different

micro-nano processed heat pipes.

Table 1 Performance of different micro/nano structured heat pipes

Processing techniques	Dimensions	Capillary wick structure	Heat transfer performance	Reference
Chemical and thermal oxidation treatment	Capillary wick: 90×40×0.5 mm^3	Copper mesh	Equivalent thermal conductivity: 2.88×10^4W/(m·K)	Li et al.[86]
Chemical treatment	Φ97.6mm	Foam copper	Minimum thermal resistance: 0.064K/W	Sun et al.[85]
Chemical treatment	Φ97.6mm×3.9mm	Evaporator: foam copper，Condenser: copper mesh	Minimum thermal resistance:0.041K/W	Wei et al.[84]
Chemical treatment	70×70×0.2 mm^3	Stainless-steel mesh	Effective thermal conductivity (K_{eff}): 11914.9 W/(m·K)	Yang et al.[130]
Chemical treatment	110×25×0.8mm^3	Sintered copper powder	K_{eff} =1943.5W/(m·K)	Sun et al.[131]
Chemical and thermal Oxidation Treatment	156×36×7.5 mm^3	Foam copper	Minimum thermal resistance: 0.0109K/W	Yang et al.[16]
Chemical and thermal Oxidation Treatment	100×15×0.27mm^3	Micro-groove and spiral woven mesh	K_{eff} : exceeding 10000W/(m·K)	Chen et al.[132]
Electrodepositio n process	100×50×0.6mm^3	Copper deposit wick	K_{eff} =12600 W/(m·K)	Luo et al.[118]
Electrodepositio n process	62.5×62.5×2 mm^3	Copper deposit wick	Lateral thermal conductivity: 6500 W/(m·K)	Yu et al.[119]
Laser process technology	80×20×0.22 mm^3	Copper micro-groove	K_{eff} =12032 W/(m·K)	Jiang et al.[13]
Laser process technology	70×70×1mm^3	Copper micro-groove	K_{eff} =17104W/(m·K)	Xie et al.[67]
Selective laser melting	60×50×4mm^3	Aluminum-based biomimetic wick	Minimum thermal resistance: 0.034K/W	Gu et al.[133]
Atomic layer deposition	20×60×0.3mm^3	All-polymer wick	K_{eff} =541 W/(m·K)	Lewis et al.[22]

Etching process	104×14×0.4mm^3	Copper mesh	K_{eff}=12000 W/(m·K)	Chen et al.[97]
Etching process	The thickness of vapor space: 0.5 mm	Silicon-based micro-grooves	Minimum thermal resistance: 1.323℃/W	Lv et al.[100]
Etching process	66×21×1.7mm^3	Silicon-based micro-grooves	Minimum thermal resistance: 1.14℃/W	Lv et al.[134]
Electrical discharge machining	/	Copper micro-groove	Minimum thermal resistance: approximately 0.3℃/W	Nishida et al.[102]

5 Conclusion and prospect

As electronic devices continue to miniaturize, the space available for cooling components becomes increasingly constrained. Efficient heat dissipation within this limited space is crucial for the operational performance and longevity of electronic devices. Consequently, extensive research has been conducted on ultra-thin heat pipes in recent years. The performance of heat pipes is significantly influenced by the capillary wick inside, which is responsible for fluid transport and heat transfer. Enhancing the vaporization of the working fluid and the return flow of the condensed fluid has been a primary focus for many researchers. The application of micro-nanofabrication techniques to achieve thin heat pipes with superior thermal performance has become a focal point of current research [135].

The following three points are used to investigate the mechanism of improving heat transfer by micro-nano structures: micro-nanostructures primarily improve surface wettability, increase the solid-liquid contact area, provide nucleation sites for vaporization, and accelerate the nucleation and removal of droplets. Most related pool boiling and condensation experiments are conducted at atmospheric pressure. However, since heat pipes operate at lower internal pressures, it is necessary to conduct boiling and condensation experiments under conditions that approximate the internal pressure of heat pipes. In addition, when applying structured surfaces designed to enhance condensation heat transfer to heat pipe condensers, it is crucial to consider the impact of vapor flow within the heat pipe.

Chemical oxidation treatments are common methods for micro-nanostructure fabrication. Compared to other methods, they do not require expensive processing equipment and can be used on sintered copper powder, copper meshes, spiral woven meshes, and porous metals. The morphology of nanostructures varies with different chemical reagents or oxidation temperatures. However, the use of strong acids/alkalis during processing poses certain hazards and environmental pollution.

Electrochemical deposition is slightly more complex than chemical/thermal oxidation. It requires precise electrolyte preparation, covering the sample with an insulating film while leaving deposition areas exposed, and controlling current and deposition time during the process.

Laser processing methods involve expensive equipment but offer the advantage of directly fabricating microstructures on the substrate to create UTHPs. The molten particles formed during processing create micro-nanostructures that enhance capillary action and heat transfer. This method requires careful control of laser scanning speed, flux, power, and repetition frequency.

Heat pipes using nanofluids demonstrate better thermal performance compared to those using deionized water. During heating, nanoparticles in the nanofluid deposit on the heating surface, forming a nanoparticle layer that strengthens capillary action and heat transfer. Experimental results show that different nanofluids, such as graphene and Al_2O_3 nanofluids, produce varying effects, allowing the selection of appropriate nanofluids based on working conditions. This paper focuses on the improvement of internal surface structures of heat pipes using nanofluids. The mechanisms of nanofluid-enhanced heat transfer in heat pipes include: enhancement of wall-to-fluid convective heat transfer[136], thermal properties of nanofluids[137], and Brownian motion of nanoparticles in fluids[138]. Considering the role of nanoparticle layers, PVD can deposit uniform and controllable thickness nanoparticle layers on surfaces, providing an alternative to using nanofluids.

Recent research on cooling issues for foldable devices has expanded significantly. While metals offer good thermal conductivity, metal fatigue due to prolonged folding is a notable problem. Polymers, compared to metals, exhibit greater flexibility. Heat pipes with polymer wicks, after hydrophilic treatment, can enhance thermal performance, but the thermal conductivity of polymers is much lower than that of copper/aluminum, resulting in lower effective thermal conductivity of the fabricated heat pipes. Graphene-based composites, with their high thermal conductivity and mechanical strength, present a promising approach to addressing the low thermal conductivity of flexible heat pipes. Hu et al.[139] incorporated graphene oxide sheets into CNT films, after high-temperature annealing, achieved a CNT/graphene film with a mechanical strength approaching 1 GPa and a thermal conductivity of 1056 W/(m·K). In this hybrid structure, CNTs serve as robust porous support frameworks.

Direct cooling of semiconductor chips is made possible by micro heat pipes, which are made with MEMS technology and embedded into the chips themselves. Due to the small size of micro heat pipes, their manufacturing process is more complex and demanding. Fabrication techniques include wet etching or DRIE to create microgrooves or other complex microstructures on silicon wafers. Achieving vacuum conditions to meet pressures between 10^{-4} and 10^{-2} torr is essential. Additionally, accurately controlling the fill volume is a significant challenge, as the total liquid volume required for micro heat pipes is approximately 10-100 μL[140], necessitating the development of precision filling devices.

Electric discharge machining can directly machine high aspect ratio microgrooves on the surface of the substrate, with a machining accuracy of up to 1 μm[95]. It is considered one of the ideal methods for manufacturing UTHPs, and the use of shaped electrodes can create complex three-dimensional microgroove capillary structures. However, this method suffers from low processing efficiency and significant electrode wear during fabrication, making it unsuitable for large-scale production. In conclusion, substantial progress has been made in the research of metal-based heat pipes with micro-nanostructures, resulting in various high-performance prototypes. Additionally, extensive research has been conducted on silicon-based

MHPs, which offer promising compatibility with electronic components and excellent thermal performance. However, further study is required on flexible polymer heat pipes, with a focus on material outgassing difficulties with polymer shells, the low thermal conductivity of polymer wicks, and fatigue issues with metal wick flexible polymer heat pipes. Moreover, the durability of micro-nanostructures on heat pipe surfaces over time is a concern. Improving processing techniques or exploring new technologies to enhance the longevity of nanostructures is crucial for maintaining heat pipe performance.

Acknowledgments

The supports of our research program by National Natural Science Foundation of China (No. 52276155), Key Laboratory of Aero-engine Thermal Environment and Structure, Ministry of Industry and Information Technology (CEPE2022003) are greatly appreciated.

References

[1] Ball, P., Computer engineering: Feeling the heat, *Nature*, *492*. (2012), 7428, pp. 174-176
[2] Balandin, A.A., *et al.*, Superior Thermal Conductivity of Single-Layer Graphene, *Nano Letters*, *8*. (2008), 3, pp. 902-907
[3] Li, Z., *et al.*, Facile Synthesis of a Graphene Film with Ultrahigh Thermal Conductivity via a Novel Pressure-Swing Hot-Pressing Method, *Industrial & Engineering Chemistry Research*, *63*. (2024), 10, pp. 4442-4450
[4] Shaeri, M.R., *et al.*, Vapor chambers with hydrophobic and biphilic evaporators in moderate to high heat flux applications, *Applied Thermal Engineering*, *130*. (2018), pp. 83-92
[5] Huang, G., *et al.*, Fabrication and thermal performance of mesh-type ultra-thin vapor chambers, *Applied Thermal Engineering*, *162*. (2019), p. 114263
[6] Liu, T., *et al.*, Improving the thermal performance of thin vapor chamber by optimizing screen mesh wick structure, *Thermal Science and Engineering Progress*, *36*. (2022), p. 101535
[7] Zhang, X., *et al.*, Preparation method and thermal performance of a new ultra-thin flexible flat plate heat pipe, *Heat Transfer Research*, *55*. (2024), 11, pp. 1-17
[8] Zhou, W., *et al.*, Effect of the passage area ratio of liquid to vapor on an ultra-thin flattened heat pipe, *Applied Thermal Engineering*, *162*. (2019), p. 114215
[9] Zhou, W.J., *et al.*, A novel ultra-thin flattened heat pipe with biporous spiral woven mesh wick for cooling electronic devices, *Energy Conversion and Management*, *180*. (2019), pp. 769-783
[10] Tang, Y., *et al.*, Experimental investigation of capillary force in a novel sintered copper mesh wick for ultra-thin heat pipes, *Applied Thermal Engineering*, *115*. (2017), pp. 1020-1030
[11] Chang, C., *et al.*, 3D printed aluminum flat heat pipes with micro grooves for efficient thermal management of high power LEDs, *Scientific Reports*, *11*. (2021), 1, p. 8255
[12] Liu, F., *et al.*, Design and Heat Transfer Performance of Flat-Plate Heat Pipe with Leaf Veins, *Heat Transfer Research*, *54*. (2023), 11, pp. 35-50
[13] Jiang, G., *et al.*, Laser microstructuring of extremely-thin vapor chamber with hybrid configuration for excellent heat dissipation, *Energy Conversion and Management*, *290*. (2023), p. 117214
[14] Tang, H., *et al.*, Fabrication and capillary characterization of axially micro-grooved wicks for aluminium flat-plate heat pipes, *Applied Thermal Engineering*, *129*. (2018), pp. 907-915
[15] Ji, X.B., *et al.*, Copper foam based vapor chamber for high heat flux dissipation, *Experimental Thermal and Fluid Science*, *40*. (2012), pp. 93-102
[16] Yang, H.Z., *et al.*, Experimental study on thermal performance of high power flat heat pipe, *CIESC Journal*, *74*. (2023), 04, pp. 1561-1569
[17] Wang, L.Q., *et al.*, HEAT DISSIPATION PERFORMANCE OF GROOVED-TYPE AND COPPER FOAM-TYPE VAPOR CHAMBERS, *THERMAL SCIENCE*, *26*. (2022), 2, pp. 1357-1366
[18] Liu, C., *et al.*, Vapor chamber with two-layer liquid supply evaporator wick for high-heat-flux devices, *Applied Thermal Engineering*, *190*. (2021), p. 116803
[19] Li, Q., *et al.*, Fabrication and capillary characterization of multi-scale micro-grooved wicks with sintered copper powder, *International Communications in Heat and Mass Transfer*, *121*. (2021), p. 105123

[20] Zhao, Z., *et al.*, Powder sintered flat micro-heat pipe with wettability modification, *International Journal of Modern Physics B*, *36*. (2022), 06, p. 2240009
[21] Sugimoto, K., *et al. Design and Fabrication of Flexible Two-Phase Heat Transport Device for Wearable Interfaces*,2021 IEEE 34th International Conference on Micro Electro Mechanical Systems (MEMS),2021, pp. 95-98
[22] Lewis, R., *et al.*, Microfabricated ultra-thin all-polymer thermal ground planes, *Science Bulletin*, *60*. (2015), 7, pp. 701-706
[23] Tang, H., *et al.*, Pool boiling heat transfer performance of micro-embossing molds for the fabrication of polymer wicks, *Physics of Fluids*, *36*. (2024), 2, p. 023346
[24] Huang, G.W., *et al.*, Fabrication and capillary performance of a novel composite wick for ultra-thin heat pipes, *International Journal of Heat and Mass Transfer*, *176*. (2021), p. 121467
[25] Yu, J., *et al.*, Effect of spiral woven mesh liquid pumping action on the heat transfer performance of ultrathin vapour chamber, *International Journal of Thermal Sciences*, *182*. (2022), p. 107799
[26] Wong, S.-C.,W.-S. Liao, Visualization experiments on flat-plate heat pipes with composite mesh-groove wick at different tilt angles, *International Journal of Heat and Mass Transfer*, *123*. (2018), pp. 839-847
[27] Huang, G., *et al.*, Optimizing L-shaped heat pipes with partially-hybrid mesh-groove wicking structures, *International Journal of Heat and Mass Transfer*, *170*. (2021), p. 120926
[28] Yan, C., *et al.*, A novel ultra-thin vapor chamber with composite wick for portable electronics cooling, *Applied Thermal Engineering*, *226*. (2023), p. 120340
[29] Wang, J., *et al.*, Rice-inspired oriented copper fiber wick with excellent capillary performance for ultra-thin vapor chamber, *Applied Thermal Engineering*, *236*. (2024), p. 121573
[30] Zheng, S., *et al.*, Study on the thermal performance of pulmonary vascular-inspired grooved vapor chamber, *Applied Thermal Engineering*, *242*. (2024), p. 122545
[31] Damoulakis, G.,C.M. Megaridis, Wick-free paradigm for high-performance vapor-chamber heat spreaders, *Energy Conversion and Management*, *253*. (2022), p. 115138
[32] Luo, Q.Y., *et al.*, Characteristics of droplet transportation on feather-shaped superhydrophilic-superhydrophobic patterns, *Surfaces and Interfaces*, *42*. (2023), p. 103460
[33] Bang, S., *et al.*, Superhydrophilic catenoidal aluminum micropost evaporator wicks, *International Journal of Heat and Mass Transfer*, *158*. (2020), p. 120011
[34] Struss, Q., *et al.*, Design and fabrication of an ultra-thin silicon vapor chamber for compact electronic cooling, *2020 Ieee 70th Electronic Components and Technology Conference (Ectc 2020)*. (2020), pp. 2259-2265
[35] Long, J., *et al.*, Dual-scale porous/grooved microstructures prepared by nanosecond laser surface texturing for high-performance vapor chambers, *Journal of Manufacturing Processes*, *73*. (2022), pp. 914-923
[36] Liu, T.Q., *et al.*, THERMAL PERFORMANCE OF WICKLESS AND ORIENTATION INDEPENDENT THIN VAPOR CHAMBERS WITH WETTABILITY PATTERNED MICRO STRUCTURE, *THERMAL SCIENCE*, *26*. (2022), 5, pp. 4391-4400
[37] Tang, H., *et al.*, Review of applications and developments of ultra-thin micro heat pipes for electronic cooling, *Applied Energy*, *223*. (2018), pp. 383-400
[38] Faegh, M.,M.B. Shafii, Experimental investigation of a solar still equipped with an external heat storage system using phase change materials and heat pipes, *Desalination*, *409*. (2017), pp. 128-135
[39] Lu, Z., *et al.*, Experimental investigation on the thermal performance of three-dimensional vapor chamber for LED automotive headlamps, *Applied Thermal Engineering*, *157*. (2019), p. 113478
[40] Zhang, S., *et al.*, Design of 3D vapor chamber for thermal management of permanent magnet synchronous motors, *Applied Thermal Engineering*, *258*. (2025), p. 124534
[41] Wang, W.-W., *et al.*, Experimental investigation on the thermal performance of high-concentrated photovoltaic module utilizing the thermal sink of a novel Fan-shaped plate pulsating heat pipe, *Applied Energy*, *377*. (2025), p. 124365
[42] Jiang, L., *et al.*, Phase change flattening process for axial grooved heat pipe, *Journal of Materials Processing Technology*, *212*. (2012), 1, pp. 331-338
[43] Zhou, W., *et al.*, Ultra-thin flattened heat pipe with a novel band-shape spiral woven mesh wick for cooling smartphones, *International Journal of Heat and Mass Transfer*, *146*. (2020), p. 118792
[44] Sun, Y., *et al.*, Ultrathin flexible heat pipes with Microsorum fortunei structural-like wick for cooling flexible electronic devices, *International Journal of Heat and Mass Transfer*, *202*. (2023), p. 123743
[45] Zhang, X., *et al.*, Preparation and thermal properties of biomimetic polymer-based flexible ultra-thin flat heat pipe, *Applied Thermal Engineering*, *255*. (2024), p. 124048
[46] Wang, Z., *et al.*, Experimental study on heat transfer and storage of a heating system coupled with solar flat heat pipe and phase change material unit, *Journal of Energy Storage*, *73*. (2023), p. 108971

[47] He, X., *et al.*, Study on heat transfer characteristics of a dual-evaporator ultra-thin loop heat pipe for laptop cooling, *Applied Thermal Engineering*, *241*. (2024), p. 122395
[48] Cheng, J., *et al.*, Thermal performance of a lithium-ion battery thermal management system with vapor chamber and minichannel cold plate, *Applied Thermal Engineering*, *222*. (2023), p. 119694
[49] Zhao, J., *et al.*, Design and experimental study of a novel vapor chamber for proton exchange membrane fuel cell cooling, *International Journal of Heat and Mass Transfer*, *220*. (2024), p. 124949
[50] Zhao, J., *et al.*, Effect of vapor chamber on thermo-electrical characteristics of proton exchange membrane fuel cells, *Applied Energy*, *360*. (2024), p. 122766
[51] Nesterov, D.A., *et al.*, Experimental investigations of flat T-shaped copper and titanium heat pipes, *Applied Thermal Engineering*, *198*. (2021), p. 117454
[52] Cai, Q.J.,A. Bhunia, High heat flux phase change on porous carbon nanotube structures, *International Journal of Heat and Mass Transfer*, *55*. (2012), 21-22, pp. 5544-5551
[53] Wen, R.F., *et al.*, Capillary-driven liquid film boiling heat transfer on hybrid mesh wicking structures, *Nano Energy*, *51*. (2018), pp. 373-382
[54] Li, C., *et al.*, Nanostructured copper interfaces for enhanced boiling, *Small*, *4*. (2008), 8, pp. 1084-1088
[55] Mantelli, M.B.H., *Thermosyphons and Heat Pipes: Theory and Applications,* Springer Nature, Switzerland, 2021
[56] Liu, X.L., *et al.*, Theoretical analysis of bubble nucleation in liquid film boiling, *International Journal of Heat and Mass Transfer*, *192*. (2022), p. 122911
[57] Dong, L.N., *et al.*, An experimental investigation of enhanced pool boiling heat transfer from surfaces with micro/nano-structures, *International Journal of Heat and Mass Transfer*, *71*. (2014), pp. 189-196
[58] Wen, R.F., *et al.*, Enhanced bubble nucleation and liquid rewetting for highly efficient boiling heat transfer on two-level hierarchical surfaces with patterned copper nanowire arrays, *Nano Energy*, *38*. (2017), pp. 59-65
[59] Long, J.Y., *et al.*, Highly efficient pool boiling heat transfer on surfaces with zoned rose-petal-inspired hierarchical structures, *Applied Thermal Engineering*, *241*. (2024), p. 122330
[60] Ahn, H.S.,M.H. Kim, The Effect of Micro/Nanoscale Structures on CHF Enhancement, *Nuclear Engineering and Technology*, *43*. (2011), 3, pp. 205-216
[61] Wang, X.L., *et al.*, Achieving robust and enhanced pool boiling heat transfer using micro-nano multiscale structures, *Applied Thermal Engineering*, *227*. (2023), p. 120441
[62] Das, P.,A. Das, Critical Heat Flux for Boiling in Microchannels, Butterworth-Heinemann, UK, 2016
[63] Sakashita, H., et al., Chapter 3. CHF—Transition Boiling, Elsevier, Boaton, USA, 2017
[64] Wang, Z.T., *et al.*, Wicking Enhancement in Three-Dimensional Hierarchical Nanostructures, *Langmuir*, *32*. (2016), 32, pp. 8029-8033
[65] Alhosani, M.H., *et al.*, Enhanced liquid propagation and wicking along nanostructured porous surfaces, *Advanced Engineering Materials*, *23*. (2021), 7, p. 2100118
[66] Jiang, C., Fast Capillary Wicking on Hierarchical Copper Nanowired Surfaces with Interconnected V-Grooves: Implications for Thermal Management, *ACS Applied Nano Materials*, *4*. (2021), 5, pp. 5360-5371
[67] Xie, X., *et al.*, Ultrafast laser preparation of gas-liquid partitioned microgroove wicks to enhance heat transfer in ultrathin vapor chambers, *International Journal of Heat and Mass Transfer*, *224*. (2024), p. 125317
[68] Wu, Y.X., *et al.*, Enhanced capillary performance of multiscale ultrathin titanium wicks guided by modified wicking dynamics, *International Journal of Heat and Mass Transfer*, *221*. (2024), p. 125000
[69] Rose, J.W., Dropwise condensation theory and experiment: a review, *Proceedings of the Institution of Mechanical Engineers Part a-Journal of Power and Energy*, *216*. (2002), A2, pp. 115-128
[70] Upot, N.V., *et al.*, Advances in micro and nanoengineered surfaces for enhancing boiling and condensation heat transfer: a review, *Nanoscale Advances*, *5*. (2023), 5, pp. 1232-1270
[71] Ma, X., *et al.*, Wetting mode evolution of steam dropwise condensation on superhydrophobic surface in the presence of noncondensable gas, *ASME Journal of Heat Transfer*, *134*. (2012), 2, p. 021501
[72] Miljkovic, N., *et al.*, Effect of Droplet Morphology on Growth Dynamics and Heat Transfer during Condensation on Superhydrophobic Nanostructured Surfaces, *Acs Nano*, *6*. (2012), 2, pp. 1776-1785
[73] Miljkovic, N., *et al.*, Jumping-Droplet-Enhanced Condensation on Scalable Superhydrophobic Nanostructured Surfaces, *Nano Letters*, *13*. (2013), 1, pp. 179-187
[74] Wen, R.F., *et al.*, Hydrophobic copper nanowires for enhancing condensation heat transfer, *Nano Energy*, *33*. (2017), pp. 177-183
[75] Wen, R.F., *et al.*, Three-Dimensional Superhydrophobic Nanowire Networks for Enhancing Condensation Heat Transfer, *Joule*, *2*. (2018), 2, pp. 269-279
[76] Gao, S.W., *et al.*, Dropwise condensation heat transfer on vertical superhydrophobic surfaces with fractal microgrooves in steam, *International Journal of Heat and Mass Transfer*, *217*. (2023), p. 124641

[77] Wen, R.F., *et al.*, Advances in condensation heat transfer enhancement, *Journal of Tsinghua University (Science and technology)*, *61*. (2021), 12, pp. 1353-1370
[78] Tang, Y., *et al.*, Dropwise Condensate Comb for Enhanced Heat Transfer, *Acs Applied Materials & Interfaces*, *15*. (2023), 17, pp. 21549-21561
[79] Ji, X.B., *et al.*, Dropwise condensation heat transfer on superhydrophilic-hydrophobic network hybrid surface, *International Journal of Heat and Mass Transfer*, *132*. (2019), pp. 52-67
[80] Wen, R.F., *et al.*, Sustaining enhanced condensation on hierarchical mesh-covered surfaces, *National Science Review*, *5*. (2018), 6, pp. 878-887
[81] Wu, C., *et al.*, Enhanced capillary performance of nanostructures copper woven mesh wick for ultrathin heat pipes, *Applied Thermal Engineering*, *242*. (2024), p. 122476
[82] Li, X.B., *et al.*, Liquid film boiling enabled ultra-high conductance and high flux heat spreaders, *Cell Reports Physical Science*, *3*. (2022), 3, p. 100746
[83] Li, H.C., *et al.*, Investigation on the performance of bionic wick flat pipe, *Journal of Aerospace Power*, *32*. (2017), 10, pp. 2403-2409
[84] Wei, X., *et al.*, An improved vapor chamber with enhanced two-phase transport by using structured surfaces, *Applied Thermal Engineering*, *236*. (2024), p. 121507
[85] Sun, K., *et al.*, Thermal performance of a vapor chamber with synergistic effects of droplet jumping and pillared-wick capillarity, *International Journal of Heat and Mass Transfer*, *195*. (2022), p. 123167
[86] Li, J., *et al.*, Mechanism of a microscale flat plate heat pipe with extremely high nominal thermal conductivity for cooling high-end smartphone chips, *Energy Conversion and Management*, *201*. (2019), p. 112202
[87] Shum, C., *et al.*, Enhancing wicking microflows in metallic foams, *Microfluidics and Nanofluidics*, *21*. (2017), 12, p. 177
[88] Sun, Q.S., *et al.*, Characterization of high-performance nanostructured wick for heat pipes, *Applied Thermal Engineering*, *236*. (2024), p. 121814
[89] Reinhardt, H., *et al.*, Nanoscaled Fractal Superstructures via Laser Patterning-A Versatile Route to Metallic Hierarchical Porous Materials, *Advanced Materials Interfaces*, *8*. (2021), 4, p. 2000253
[90] Rajan, R.A., *et al.*, Femtosecond and picosecond laser fabrication for long-term superhydrophilic metal surfaces, *Optics and Laser Technology*, *143*. (2021), p. 107241
[91] Liu, T.Q., *et al.*, Thermal performance enhancement of vapor chamber with modified thin screen mesh wick by laser etching, *Case Studies in Thermal Engineering*, *28*. (2021), p. 101525
[92] Yuan, X.P., *et al.*, Fabrication and capillary performance of multi-scale microgroove ceramic wicks via nanosecond laser irradiation for ultrathin ceramic heat pipes, *Applied Thermal Engineering*, *236*. (2024), p. 121927
[93] Jiang, H., *et al.*, A dual-height wick to improve capillary performance of vapor chambers, *Applied Thermal Engineering*, *241*. (2024), p. 122371
[94] Lou, D., *et al.*, Novel capillary rise enhancement of dual-shape hybrid groove made by laser etch-sputtering, *Optics & Laser Technology*, *179*. (2024), p. 111261
[95] Sun, Y., *et al.*, A review on fabrication and pool boiling enhancement of three-dimensional complex structures, *Renewable and Sustainable Energy Reviews*, *162*. (2022), p. 112437
[96] Shung-Wen, K.,H. Derlin, Fabrication of star grooves and rhombus grooves micro heat pipe, *Journal of Micromechanics and Microengineering*, *12*. (2002), 5, p. 525
[97] Chen, Z., *et al.*, Design, fabrication and thermal performance of a novel ultra-thin vapour chamber for cooling electronic devices, *Energy Conversion and Management*, *187*. (2019), pp. 221-231
[98] Zhao, Y., *et al. Beetle Inspired Electrospray Vapor Chamber*,ASME 2009 Second International Conference on Micro/Nanoscale Heat and Mass Transfer,2009,ASME 2009 Second International Conference on Micro/Nanoscale Heat and Mass Transfer, Volume 3, pp. 439-441
[99] Liu, W., *et al.*, The performance of the vapor chamber based on the plant leaf, *International Journal of Heat and Mass Transfer*, *98*. (2016), pp. 746-757
[100] Lv, Y., *et al.*, Corner flow characteristics in a silicon-based ultra-thin flat-grooved heat pipe with double-end cooling, *International Journal of Thermal Sciences*, *198*. (2024), p. 108860
[101] Tang, H., *et al.*, Fabrication and pool boiling performance assessment of microgroove array surfaces with secondary micro-structures for high power applications, *Renewable Energy*, *187*. (2022), pp. 790-800
[102] Felipe, N.B., *et al.*, Experimental investigation of heat pipe thermal performance with microgrooves fabricated by wire electrical discharge machining, *Thermal Science*, *24*. (2020), pp. 701-711
[103] Zhou, R., *et al.*, Experimental study on thermal performance of copper nanofluids in a miniature heat pipe fabricated by wire electrical discharge machining, *Applied Thermal Engineering*, *160*. (2019), p. 113989

[104] Tang, H., *et al.*, Fabrication and capillary characterization of multi-scale microgroove wicks for ultrathin phase-change heat transfer devices, *Applied Thermal Engineering*, *219*. (2023), p. 119621
[105] Golubovic, M.N., *et al.*, Nanofluids and critical heat flux, experimental and analytical study, *Applied Thermal Engineering*, *29*. (2009), 7, pp. 1281-1288
[106] Okawa, T., *et al.*, Boiling time effect on CHF enhancement in pool boiling of nanofluids, *International Journal of Heat and Mass Transfer*, *55*. (2012), 9, pp. 2719-2725
[107] Ghanbarpour, M., *et al.*, Thermal performance of screen mesh heat pipe with Al_2O_3 nanofluid, *Experimental Thermal and Fluid Science*, *66*. (2015), pp. 213-220
[108] Tsai, C.Y., *et al.*, Effect of structural character of gold nanoparticles in nanofluid on heat pipe thermal performance, *Materials Letters*, *58*. (2004), 9, pp. 1461-1465
[109] Gupta, N.K., *et al.*, Experimental study of thermal performance of nanofluid-filled and nanoparticles-coated mesh wick heat pipes, *Journal of Heat Transfer*, *140*. (2018), 10, p. 102403
[110] Xu, Y., *et al.*, Molecular engineered conjugated polymer with high thermal conductivity, *Science Advances*, *4*. (2018), 3, p. eaar3031
[111] Roy, A., *et al.*, Thermal Conductance of Poly(3-methylthiophene) Brushes, *ACS Applied Materials & Interfaces*, *8*. (2016), 38, pp. 25578-25585
[112] Abdulagatov, A.I., *et al.*, Al_2O_3 and TiO_2 Atomic Layer Deposition on Copper for Water Corrosion Resistance, *ACS Applied Materials & Interfaces*, *3*. (2011), 12, pp. 4593-4601
[113] Rahman, I.A.,V. Padavettan, Synthesis of Silica nanoparticles by Sol-Gel: Size-dependent properties, surface modification, and applications in silica-polymer nanocompositesa review, *Journal of nanomaterials*. (2012), Pt.3, p. 2012
[114] Orazi, L., *et al.*, Ultrafast laser texturing to improve wettability of polyimide (Kapton) films, *Journal of Manufacturing Processes*, *107*. (2023), pp. 368-375
[115] Tang, Y., *et al.*, Enhanced capillary performance of ultrathin nylon mesh wick for flexible thermal management systems, *International Journal of Heat and Mass Transfer*, *200*. (2023), p. 123545
[116] Nikolić, N.D., *et al.*, Morphologies of copper deposits obtained by the electrodeposition at high overpotentials, *Surface and Coatings Technology*, *201*. (2006), 3, pp. 560-566
[117] Wen, R.F., *et al.*, Hierarchical Superhydrophobic Surfaces with Micropatterned Nanowire Arrays for High-Efficiency Jumping Droplet Condensation, *Acs Applied Materials & Interfaces*, *9*. (2017), 51, pp. 44911-44921
[118] Luo, J., *et al.*, Biomimetic Copper Forest Wick Enables High Thermal Conductivity Ultrathin Heat Pipe, *ACS Nano*, *15*. (2021), 4, pp. 6614-6621
[119] Yu, J.C., *et al.*, High-performance electrodeposited copper wicks for heat-spreading vapor chambers, *Applied Thermal Engineering*, *228*. (2023), pp. 1-9
[120] Chen, Q.,Y. Huang, Scale effects on evaporative heat transfer in carbon nanotube wick in heat pipes, *International Journal of Heat and Mass Transfer*, *111*. (2017), pp. 852-859
[121] Cai, Q.,C.L. Chen, Design and Test of Carbon Nanotube Biwick Structure for High-Heat-Flux Phase Change Heat Transfer, *Journal of Heat Transfer*, *132*. (2010), 5, p. 052403
[122] Cai, Q.,A. Bhunia, High heat flux phase change on porous carbon nanotube structures, *International Journal of Heat and Mass Transfer*, *55*. (2012), 21, pp. 5544-5551
[123] Kousalya, A.S., *et al.*, Metal functionalization of carbon nanotubes for enhanced sintered powder wicks, *International Journal of Heat and Mass Transfer*, *59*. (2013), pp. 372-383
[124] Lee, S., *et al.*, Layer-by-layer assembled carbon nanotube-polyethyleneimine coatings inside copper-sintered heat pipes for enhanced thermal performance, *Carbon*, *140*. (2018), pp. 521-532
[125] Chen, G.L.,C.H. Li, Combined effects of liquid wicking and hydrodynamic instability on pool boiling critical heat flux by two-tier copper structures of nanowires and microgrooves, *International Journal of Heat and Mass Transfer*, *129*. (2019), pp. 1222-1231
[126] Lu, L., *et al.*, Influence of electrochemical deposition parameters on capillary performance of a rectangular grooved wick with a porous layer, *International Journal of Heat and Mass Transfer*, *109*. (2017), pp. 737-745
[127] Sudhan, A.L.S., *et al.*, Heat transport limitations and performance enhancement of anodized grooved heat pipes charged with ammonia under gravity and anti-gravity condition, *Applied Thermal Engineering*, *200*. (2022), p. 117633
[128] Li, J.,M. Zhang, Enhanced capillary performance of grooved nanocarbon foams as wicks for heat pipes, *International Communications in Heat and Mass Transfer*, *130*. (2022), p. 105763
[129] He, H., *et al.*, Preparation of hierarchical microgroove textures on the surface of Al-based wicks by roller pressing and laser scanning irradiation, *Surface and Coatings Technology*, *487*. (2024), p. 131008

[130] Yang, Y.C., *et al.*, Microstructured wettability pattern for enhancing thermal performance in an ultrathin vapor chamber, *Case Studies in Thermal Engineering*, *25*. (2021), p. 100906
[131] Sun, Y.L., *et al.*, Ultrathin flexible heat pipes with Microsorum fortunei structural-like wick for cooling flexible electronic devices, *International Journal of Heat and Mass Transfer*, *202*. (2023), p. 123743
[132] Chen, G., *et al.*, Vapor-liquid coplanar structure enables high thermal conductive and extremely ultrathin vapor chamber, *Energy*, *301*. (2024), p. 131689
[133] Gu, Z., *et al.*, Enhancing heat transfer performance of aluminum-based vapor chamber with a novel bionic wick structure fabricated using additive manufacturing, *Applied Thermal Engineering*, *247*. (2024), p. 123076
[134] Lv, Y., *et al.*, Liquid plug characteristics and heat transfer performance of a silicon-based ultra-thin flat heat pipe at different incline angles, *Applied Thermal Engineering*, *253*. (2024), p. 123702
[135] Filippou, I., *et al.*, A review of microfabrication approaches for the development of thin, flattened heat pipes and vapor chambers for passive electronic cooling applications, *Micro and Nano Engineering*, *22*. (2024), p. 100235
[136] Kumaresan, G., *et al.*, Experimental investigation on enhancement in thermal characteristics of sintered wick heat pipe using CuO nanofluids, *International Journal of Heat and Mass Transfer*, *72*. (2014), pp. 507-516
[137] Liu, Z.,Q. Zhu, Application of aqueous nanofluids in a horizontal mesh heat pipe, *Energy Conversion and Management*, *52*. (2011), 1, pp. 292-300
[138] Liu, Z.-H., *et al.*, Compositive effect of nanoparticle parameter on thermal performance of cylindrical micro-grooved heat pipe using nanofluids, *International Journal of Thermal Sciences*, *50*. (2011), 4, pp. 558-568
[139] Hu, D., *et al.*, Strong graphene-interlayered carbon nanotube films with high thermal conductivity, *Carbon*, *118*. (2017), pp. 659-665
[140] Qu, J., *et al.*, Recent advances in MEMS-based micro heat pipes, *International Journal of Heat and Mass Transfer*, *110*. (2017), pp. 294-313

Submitted: 04.11.2024.
Revised: 22.12.2024.
Accepted: 13.03.2025.